

# Characterizing Quantum-Dot Cellular Automata

Burkhard Ritter  
Supervised by Prof. Dr. Kevin Beach

May 2014



# Contents

<b>1</b>	<b>Approximations</b>	<b>5</b>
1.1	Fixed charge model . . . . .	5
1.2	Bond model . . . . .	6
1.3	Ising model . . . . .	7
1.4	Validity of the approximations . . . . .	13



# Chapter 1

## Approximations

### 1.1 Fixed charge model

Exact diagonalization scales exponentially with system size. For the full *grand canonical* QCA Hamiltonian, Eq. ??, only QCA devices of up to two cells are computationally feasible. Therefore, to access larger systems we need to introduce approximations. Approximating means to simplify. However, by carefully establishing successive approximations and their limits, we also reduce the problem to its essential ingredients and thus, hopefully, we gain a better understanding of the system. As a first step, we reduce the Hilbert space to a *fixed* number of particles per cell. We disallow any charge fluctuations, both for the system as a whole and for each individual cell. With that, we omit the chemical potential term in the Hamiltonian,  $\mu = 0$ , and prohibit inter-cell hopping. This is a major simplification. However, it is in line with the QCA idea: The approach requires a fixed number of charges per cell, typically two electrons, and cells are thought to interact only via Coulomb forces. In a sense we are shifting the starting point of our investigation. If the *fixed* charge approximation is not valid for a given system, then there is no hope of implementing QCA on it. On the other hand, for experimental systems like the atomic silicon quantum dots and for a given cell layout, it should always be possible, at least in principle, to tune the system parameters, especially the chemical potential, to get the system into the right particle number sector. The system has to be set up in a way that the two-electrons-per-cell sector is lowest in energy and other particle number sectors are sufficiently gapped out, that is, at an energy, compared to the ground state energy, much larger than temperature. Of course, in practice there are very clear limits as to how much the system parameters can be tuned and any QCA cell layout considered within the *fixed* charge approximation cannot necessarily be readily implemented on a given real-world material system.

For the *fixed* charge system, the state space scales as  $N_s = \binom{8}{2}^{N_c} = 28^{N_c}$  ( $N_c$  is the number of cells). Using symmetries, the largest block of the Hamiltonian matrix is the spin zero sector, of size  $N'_s = 16^{N_c}$ . On conventional computer hardware, systems of

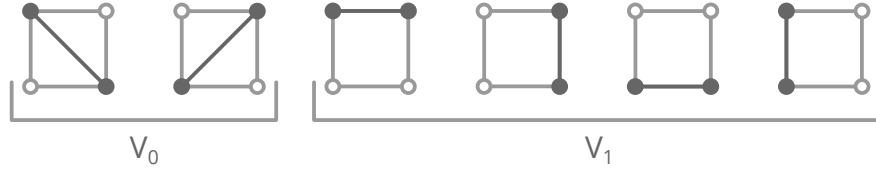


Figure 1.1: ...

up to four cells are possible, with memory requirements of 32GB. In practice, however, calculations for four-cell systems take too long and thus three cells is the practical limit for the *fixed*-number-of-particles-per-cell model.

## 1.2 Bond model

At its heart, QCA is a semi-classical idea. It relies solely on charge-charge interactions and ignores the particle spins. Therefore, as a next step in our quest to access larger system sizes, we neglect the spin degree of freedom in our model. The 28 states per cell of the *fixed* charge model can be reorganized into four doubly occupied dots and six bonds. The six bonds are illustrated in Fig. 1.1. Each bond corresponds to one spin singlet and three spin triplet states. The *bond* approximation only keeps one state for each bond and discards the doubly occupied states as well. With the *bond* model we thus assume that singlet and triplet states are qualitatively equivalent and energetically degenerate, and that doubly occupied dots are sufficiently gapped out, that is,  $U \gg T$ . As QCA ignores the spin, singlets and triplets should be qualitatively equivalent, but they are not quite degenerate. We expect that virtual double-occupancy lowers the energies of the singlet states and therefore introduces a small singlet-triplet splitting. Still, degeneracy is presumably not a bad assumption to start with and we will look at the singlet-triplet splitting in detail in due course. For the *bond* model the QCA Hamiltonian reduces to

$$H = - \sum_{\langle ij \rangle} t c_i^\dagger c_j + \sum_{i < j} V_{ij} (n_i - q) (n_j - q) . \quad (1.1)$$

With six bond states per cell, the Hilbert space of the *bond* model is  $N_s = 6^{N_c}$  ( $N_c$  the number of cells). Five and six cells are doable, with memory requirements of 460MB and 16GB, respectively, but for practical calculations five cells really is the limit. For the *bond* model there are no symmetries that can be exploited.

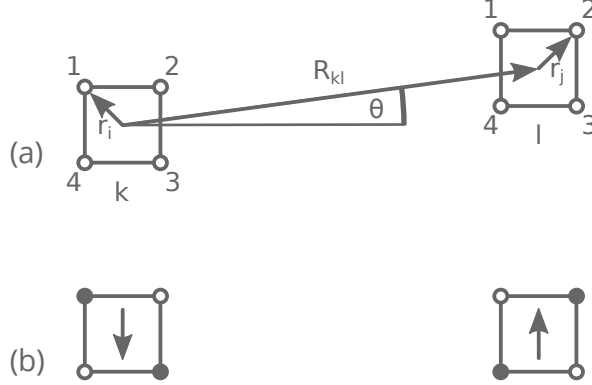


Figure 1.2: a) QCA cells  $k$  and  $l$ . b) The two-states-per-cell approximation identifies each cell with a spin  $\uparrow$  or  $\downarrow$ .

### 1.3 Ising model

A linear array of QCA cells where each cell has a state of logic 0 or 1 is reminiscent of a 1D spin  $\frac{1}{2}$  chain. Indeed, if we reduce the basis to only two states per cell, down from six states in the *bond* picture, we can map the QCA system to a transverse-field Ising model with long-ranging interactions. This is an attractive proposition: The smaller Hilbert space allows for larger system sizes with our exact diagonalization method; more importantly, the transverse-field Ising model is amenable to sign-problem-free Stochastic series expansion (SSE) quantum Monte Carlo schemes [1]. These methods do not scale exponentially<sup>1</sup> and consequently allow access to much larger systems. Last, but not least, such a mapping connects the QCA approach to the established and well studied Ising model. The prospect hinges on the assumption that the two-states-per-cell basis actually is a good approximation for QCA systems. And while bistable two-state cells are certainly the picture we have in mind when we talk about QCA, it is not *a priori* clear whether this is a correct physical picture.

We use the *bond* Hamiltonian (1.1) as the starting point. We had already discussed in the last chapter that such a Hamiltonian can be decomposed into single-cell terms and cell-cell interaction terms,

$$H = \sum_k H_k^c + \sum_{k < l} H_{kl}^{cc}. \quad (1.2)$$

In comparison, the transverse field Ising model is described by

$$\tilde{H} = - \sum_k \gamma S_k^x + \sum_{k < l} J_{kl} S_k^z S_l^z. \quad (1.3)$$

---

<sup>1</sup>SSE quantum Monte Carlo methods roughly scale as  $N \ln N$  where  $N$  is the system size.

Thus, we would like to map the single cell term  $H_k^c$  to the transverse field term  $-\gamma S_k^x$  and the Coulombic cell-cell interaction  $H_{kl}^{cc}$  to the Ising term  $J_{kl} S_k^z S_l^z$ . Each cell  $k$  is identified with a pseudo spin  $S_k^z$ , specifically the logic 0 with a spin down state and the logic 1 with a spin up state, as illustrated in Fig. 1.2(b). We will first look at how the QCA cell can be represented by only two states and derive an approximate expression for the transverse field  $\gamma$ . Then we will use a multipole expansion to derive  $J_{kl}$  from the cell-cell Coulomb interaction.

To arrive at a single-cell-basis with only two states we can, in principle, follow a similar prescription as for the fixed charge and bond approximations: We neglect high energy states which are assumed to be gapped out. In this case these are the four edge states with Coulomb energy  $V_1$ ,  $|\psi_Q\rangle = \{|3\rangle, |4\rangle, |5\rangle, |6\rangle\}$  in Fig. 1.1, where we have introduced  $|\psi_Q\rangle$  to denote the high-energy subspace of the single-cell Hilbert space. We only keep the low-energy, diagonal states  $|\psi_P\rangle = \{|1\rangle, |2\rangle\}$  with Coulomb energy  $V_0$ . Of course, these two are exactly our logic 0 and logic 1 state, or  $|1\rangle \doteq |\downarrow\rangle$  and  $|2\rangle \doteq |\uparrow\rangle$ , respectively. Here,  $|\psi_P\rangle$  denotes the low-energy subspace. For the high-energy states to be sufficiently gapped out we require  $\Delta V = V_1 - V_0 \gg T$ . In contrast to the fixed charge and bond models, merely truncating the Hilbert space is not sufficient for the Ising model. For our previous two approximations the Hamiltonian had remained essentially unchanged, apart from dropping no longer relevant terms, such as the chemical potential term or the Hubbard  $U$  term. The retained states were exactly the same states as in the full, untruncated model. But with only two states per cell the existing Hamiltonian (1.1) does not “work”: There is no process that takes the system from state  $|1\rangle$  to  $|2\rangle$ . Therefore, for the Ising approximation we need to derive an effective, low-energy Hamiltonian from the bond model. In the bond picture, for the system to transition from state  $|1\rangle$  to  $|2\rangle$  it can take different paths, for example  $|1\rangle \rightarrow |3\rangle \rightarrow 2$ , consisting of two hopping processes with an interim high-energy edge state. We will treat those processes perturbatively, as *virtual* excitations, and derive an effective hopping term between the two states  $|1\rangle$  and  $|2\rangle$ . This effective hopping term is precisely the transverse field  $\gamma$  which flips the spin in the Ising picture,  $-\gamma S_k^x = -\gamma \frac{1}{2} (S_k^+ + S_k^-)$ .

A single QCA cell is described by the time-independent Schrödinger equation  $H_k^c |\psi\rangle = E_k |\psi\rangle$ , with  $|\psi\rangle = [|\psi_P\rangle, |\psi_Q\rangle]$ . Our aim is to truncate the basis to  $|\psi_P\rangle$  and derive an effective Hamiltonian  $\tilde{H}_k^c$  with the subspace Schrödinger equation  $\tilde{H}_k^c |\psi_P\rangle = E_k |\psi_P\rangle$ . The high-energy states  $|\psi_Q\rangle$  have to be incorporated as virtual excitations. Using the basis depicted in Fig. 1.1 the single-cell bond Hamiltonian is very simple and can be written down explicitly. As the single-cell Hamiltonian is the same for all cells, we can drop the



index  $k$ .

$$\begin{aligned}
 H^c &= \left( \begin{array}{cc|cccc} V_0 & 0 & -t & -t & -t & -t \\ 0 & V_0 & -t & -t & -t & -t \\ \hline -t & -t & V_1 & 0 & 0 & 0 \\ -t & -t & 0 & V_1 & 0 & 0 \\ -t & -t & 0 & 0 & V_1 & 0 \\ -t & -t & 0 & 0 & 0 & V_1 \end{array} \right) \\
 &= \begin{pmatrix} H_{PP} & H_{PQ} \\ H_{QP} & H_{QQ} \end{pmatrix}
 \end{aligned} \tag{1.4}$$

Here, we have partitioned the Hamiltonian into four blocks,  $H_{PP}$ ,  $H_{QQ}$ ,  $H_{PQ}$ , and  $H_{QP}$ , corresponding to the low-energy subspace  $|\psi_P\rangle$ , the high-energy subspace  $|\psi_Q\rangle$ , and transitioning between the subspaces. With a this partitioned Hamiltonian the time-independent Schrödinger equation is

$$\begin{pmatrix} H_{PP} & H_{PQ} \\ H_{QP} & H_{QQ} \end{pmatrix} \begin{pmatrix} \psi_P \\ \psi_Q \end{pmatrix} = E \begin{pmatrix} \psi_P \\ \psi_Q \end{pmatrix} \tag{1.5}$$

Writing out the matrix equation as two equations explicitly and eliminating  $|\psi_Q\rangle$  yields

$$H_{PP} |\psi_P\rangle + H_{PQ} \frac{1}{E - H_{QQ}} H_{QP} |\psi_P\rangle = E |\psi_P\rangle \tag{1.6}$$

and therefore

$$\tilde{H}^c = H_{PP} + H_{PQ} \frac{1}{E - H_{QQ}} H_{QP}. \tag{1.7}$$

Assuming that the system is predominantly in the subspace spanned by  $|\psi_P\rangle$  and additionally that the hopping is very small,  $t \ll V_0$ , we can approximate  $E \approx V_0$ . We write out the matrix multiplications and use  $H_{PP} = (V_0)_{ii} \delta_{ij}$ ,  $H_{PQ} = (-t)_{ij}$ , and so on. The effective Hamiltonian becomes

$$\begin{aligned}
 \tilde{H}_{ij}^c &= (V_0)_{ii} \delta_{ij} + (-t)_{ik} (V_0 - V_1)_{kk}^{-1} (-t)_{kj} \\
 &= (V_0)_{ii} \delta_{ij} - \left( \frac{4t^2}{\Delta V} \right)_{ij}.
 \end{aligned} \tag{1.8}$$

As the system remains unchanged upon adding a constant term to the Hamiltonian, we can subtract the constant diagonal term  $\tilde{H}_{ii} = V_0 - \frac{4t^2}{\Delta V}$ , and arrive at

$$\tilde{H}^c = \begin{pmatrix} 0 & -\frac{4t^2}{\Delta V} \\ -\frac{4t^2}{\Delta V} & 0 \end{pmatrix}. \tag{1.9}$$

The off-diagonal matrix elements are the effective hopping, transitioning the system between its two states  $|1\rangle \leftrightarrow |2\rangle$ . If we now compare this matrix with the transverse field term of the Ising model, where we use the basis  $|\downarrow\rangle \doteq |1\rangle$  and  $|\uparrow\rangle \doteq |2\rangle$ ,

$$\begin{aligned}\tilde{H}^c &= -\gamma S_k^x \\ &= -\frac{1}{2}\gamma (S_k^+ + S_k^-) \\ &= \begin{pmatrix} 0 & -\frac{1}{2}\gamma \\ -\frac{1}{2}\gamma & 0 \end{pmatrix},\end{aligned}\tag{1.10}$$

we identify the effective hopping as the transverse field  $\gamma$

$$\gamma = \frac{8t^2}{\Delta V}.\tag{1.11}$$

The effective hopping  $\gamma$  is a virtual process, involving two hopping processes in the original bond model, yielding the  $t^2$  in the numerator of the expression for  $\gamma$ , and an interim high-energy state gapped out by  $\Delta V$ , hence the  $\Delta V$  in the denominator. To arrive at the expression for the effective hopping we used the assumptions  $\Delta V \gg T$  and  $t \ll \Delta V$ . As a reminder,  $\Delta V = V_1 - V_0 = \frac{2-\sqrt{2}}{2}\frac{1}{a} \approx 0.3V_1$ . Notably, the energy gap is independent of the compensation charge  $q$ . As the derivation used only a single cell, it is also implicitly assumed that the perturbations from other cells in the system are small, at least as far as the effective hopping is concerned. If the hopping depended on nearby cells' state, then the effective Hamiltonian would be much more involved and certainly could not be mapped to an Ising-like model.

We have successfully derived an effective hopping term and therefore also an effective two-state model for the QCA Hamiltonian. With only two states per cell the Hilbert space scales as  $N_s = 2^{N_c}$  ( $N_c$  the number of cells) and up to 14 cells are computationally feasible, with memory requirements of 2GB. In practice we restrict the calculations to a maximum of 12 or 13 cells. For our calculations we can use the two-state approximation with the effective hopping term, but still retain the original cell-cell interaction term  $H_{kl}^{cc}$ . Summing up all cell-cell interactions exactly is no problem for the relatively small system sizes accessible with exact diagonalization. Thus, from a computational point of view, nothing is gained by expressing the cell-cell interaction as an Ising interaction. However, deriving  $J_{kl}$  from  $H_{kl}^{cc}$  is very rewarding conceptually and enables us to properly map the QCA approach to an Ising model. Additionally, an analytical expression for  $J_{kl}$  will already allow some key insights into the characteristics of QCA devices. Therefore, we now undertake the derivation of an expression for  $J_{kl}$ . The obvious starting point is the cell-cell interaction

term  $H_{kl}^{cc}$ ,

$$\begin{aligned}
H_{kl}^{cc} &= \sum_{\substack{i \in k \\ j \in l}} V_{ij} (n_i - q) (n_j - q) \\
H_{kl}^{cc} &= \sum_{\substack{i \in k \\ j \in l}} \frac{(n_i - q) (n_j - q)}{|\mathbf{R}_{kl} + \mathbf{r}_j - \mathbf{r}_i|} \\
&= \sum_{\substack{i \in k \\ j \in l}} \frac{n_i n_j - q(n_i + n_j)}{|\mathbf{R}_{kl} + \mathbf{r}_{ij}|},
\end{aligned} \tag{1.12}$$

where  $i$  and  $j$  sum over the four dots  $1 \dots 4$  of cell  $k$  and  $l$ , respectively,  $\mathbf{R}_{kl}$  denotes the vector between the centres of the cells, see Fig. 1.2(a). We have introduced  $\mathbf{r}_{ij} = \mathbf{r}_j - \mathbf{r}_i$  and dropped the constant  $q^2$  term. There are only four possible configurations for two interacting cells:  $\uparrow\uparrow$ ,  $\downarrow\downarrow$ ,  $\uparrow\downarrow$ , and  $\downarrow\uparrow$ . Using the shorthand notations  $V_{ij} = \frac{1}{|\mathbf{R}_{kl} + \mathbf{r}_{ij}|} + \frac{1}{|\mathbf{R}_{kl} - \mathbf{r}_{ij}|}$  and  $V_{00} = \frac{1}{|\mathbf{R}_{kl}|}$ , we calculate their energies explicitly.

$$E^{\uparrow\uparrow} = (1 - 2q) (2V_{00} + V_{24}) - q (2V_{12} + 2V_{14}) \tag{1.13}$$

$$E^{\downarrow\downarrow} = (1 - 2q) (2V_{00} + V_{13}) - q (2V_{12} + 2V_{14}) \tag{1.14}$$

$$E^{\uparrow\downarrow} = (1 - 2q) (V_{12} + V_{14}) - q (4V_{00} + V_{13} + V_{24}) \tag{1.15}$$

$$E^{\downarrow\uparrow} = (1 - 2q) (V_{12} + V_{14}) - q (4V_{00} + V_{13} + V_{24}) \tag{1.16}$$

Note that the expression for two spin-down cells can be obtained from the expression for two spin-up cells (and similarly ( $E^{\uparrow\downarrow}$  from  $E^{\downarrow\uparrow}$ ) simply by rotating the system by  $90^\circ$ , or equivalently by permuting the dot numbering,  $1, 2, 3, 4 \rightarrow 4, 1, 2, 3$ . Symmetries can be exploited, for example  $V_{43} = V_{12}$ . Evidently,  $E^{\uparrow\downarrow} = E^{\downarrow\uparrow}$ , which, given the highly symmetric geometry of those cell arrangements, does not come as a surprise. But crucially, we find  $E^{\uparrow\uparrow} \neq E^{\downarrow\downarrow}$ . Therefore we have a system with three distinct energy levels which we cannot hope to represent with the solely two-level Ising term  $J_{kl} S_l^z S_l^z$ . Instead, let us try to map to a *modified* Ising model with a three-level cell-cell interaction term of the form

$$\tilde{H}_{kl}^{cc} = J_{kl} S_k^z S_l^z + J'_{kl} (S_k^z + S_l^z). \tag{1.17}$$

For this Hamiltonian we have the energies

$$\tilde{E}^{\uparrow\uparrow} - \tilde{E}^{\downarrow\downarrow} = 2J_{kl} + 2J'_{kl} \tag{1.18}$$

$$\tilde{E}^{\downarrow\downarrow} - \tilde{E}^{\uparrow\downarrow} = 2J_{kl} - 2J'_{kl} \tag{1.19}$$

which yields

$$J_{kl} = \frac{1}{4} (\tilde{E}^{\uparrow\uparrow} + \tilde{E}^{\downarrow\downarrow} - 2\tilde{E}^{\uparrow\downarrow}) \tag{1.20}$$

$$J'_{kl} = \frac{1}{4} (\tilde{E}^{\uparrow\uparrow} - \tilde{E}^{\downarrow\downarrow}), \tag{1.21}$$

and therefore, identifying  $E^{\uparrow\uparrow} = \tilde{E}^{\uparrow\uparrow}$ ,  $E^{\downarrow\downarrow} = \tilde{E}^{\downarrow\downarrow}$ , and so on,

$$J_{kl} = \frac{1}{4} (4V_{00} + V_{13} + V_{24} - 2V_{12} - 2V_{14}) \quad (1.22)$$

$$J'_{kl} = \frac{1}{4} (1 - 2q) (V_{24} - V_{13}) . \quad (1.23)$$

These results, while abstract, are remarkable in two ways. First, the newly introduced term  $J'_{kl}$  vanished for  $q = \frac{1}{2}$ . In this case  $E^{\uparrow\uparrow} = E^{\downarrow\downarrow}$ . Thus, for charge neutral cells we recover the genuine, unmodified transverse field Ising model. Second, the Ising  $J_{kl}$  itself is independent of the compensation charge  $q$ . We will see that  $J_{kl}$  is the quadrupole-quadrupole cell interaction, to leading order. In a sense, it captures the pure QCA interaction. With the above equations we can also already look at rotational symmetries of  $J_{kl}$  and  $J'_{kl}$ :  $J_{kl}$  is invariant under rotations by  $90^\circ$  as can be seen by permuting the dots  $1, 2, 3, 4 \rightarrow 4, 1, 2, 3$ . This is what we expect intuitively. For example, a horizontal straight line of cells ( $\theta = 0^\circ$ ) should behave exactly the same as a vertical straight line of cells ( $\theta = 90^\circ$ ). In contrast,  $J'_{kl}$  is not invariant under rotations by  $90^\circ$ . In fact, applying the same dot permutation yields  $J'_{kl} \xrightarrow{90^\circ} -J'_{kl}$ . Consequently,  $J'_{kl}$  is symmetric under rotations by  $180^\circ$ . It is also clear that a non-zero  $J'_{kl}$  breaks the system's symmetry under spin rotation, that is,  $\tilde{H}_{kl}^{cc}$  from Eq. (1.17) is not unchanged under  $\uparrow\uparrow \rightarrow \downarrow\downarrow$ . This has profound implications for QCA. For non-zero  $J'_{kl}$  we would, for example, expect different polarization responses for two spin-down cells versus two spin-up cells. From an application point of view this is definitely not what we want. For QCA operation we therefore require charge neutral cells and a genuine, unmodified Ising model.

To obtain more tangible expressions for  $J_{kl}$  and  $J'_{kl}$  we do a multipole expansion of the  $V_{ij}$  terms. Specifically,

$$\begin{aligned} \frac{1}{|\mathbf{R}_{kl} \pm r_{ij}|} &= \frac{1}{R} \left( 1 \pm 2 \frac{\mathbf{r}_{ij} \cdot \hat{\mathbf{R}}}{R} + \frac{r_{ij}^2}{R^2} \right)^{-1/2} \\ &= \frac{1}{R} (1 \pm x + y)^{-1/2} \end{aligned} \quad (1.24)$$

is Taylor-expanded in  $x$  and  $y$ , keeping all terms up to  $\mathcal{O}\left(\frac{a^4}{R^5}\right)$ , which corresponds to quadrupole-quadrupole interactions. Plugging the results of the expansion back into Eq. (1.22) and (1.23) yields

$$J_{kl} = \frac{1}{32} (9 - 105 \cos 4\theta) \frac{a^4}{R_{kl}^5} \quad (1.25)$$

$$J'_{kl} = (1 - 2q) \left( \frac{3}{2} \sin 2\theta \frac{a^2}{R_{kl}^3} + \frac{5}{4} \sin 2\theta \frac{a^4}{R_{kl}^5} \right) . \quad (1.26)$$

The leading order term of  $J_{kl}$  is  $R^{-5}$ , the quadrupole-quadrupole interaction. In contrast, the leading order term of  $J'_{kl}$  is  $R^{-3}$  and therefore, in general,  $J'_{kl}$  would be the dominating

term—yet another argument why a non-zero  $J'_{kl}$  is highly undesirable for functioning QCA devices. Of course, we find our general symmetry observations confirmed by these more concrete expressions for  $J_{kl}$  and  $J'_{kl}$ : The former is invariant under  $90^\circ$  rotations, the latter only under rotations of  $180^\circ$ . Both terms vanish at select angles. For example, we have  $J'_{kl} = 0$  for  $\theta = 0^\circ$ , so that at least for an exactly straight line of cells we recover the unmodified Ising model, even for non-charge-neutral cells. This does not help when building more complex devices than a wire, of course, but might still be useful for some experiments. As another example,  $J_{kl} = 0$  for  $\theta = 22.5^\circ$ . Conceivably, this could be exploited for device applications, to decouple closely spaced cells. As multipole expansions the obtained expressions for  $J_{kl}$  and  $J'_{kl}$  should be valid for large cell-cell distances  $R$ . In principle, an arbitrary number of higher order terms can be included to make the expressions as exact as desired. In practice on the computer, however, we do not use the multipole expansion at all, but simply sum up all Coulomb interactions exactly. We will see in due course that for the small cell-cell distances we are typically interested in, an expansion up to  $R^{-5}$  is indeed not sufficient, and higher order terms would have to be included.

In summary, with the expressions for  $J_{kl}$  and  $J'_{kl}$ , (1.25) and (1.26), together with the earlier derived  $\gamma$ , Eq. (1.11), we have successfully mapped the QCA bond Hamiltonian (1.1) to a modified transverse field Ising model

$$\tilde{H} = - \sum_k \gamma S_k^x + \sum_{k < l} [J_{kl} S_k^z S_l^z + J'_{kl} (S_k^z + S_l^z)] . \quad (1.27)$$

## 1.4 Validity of the approximations

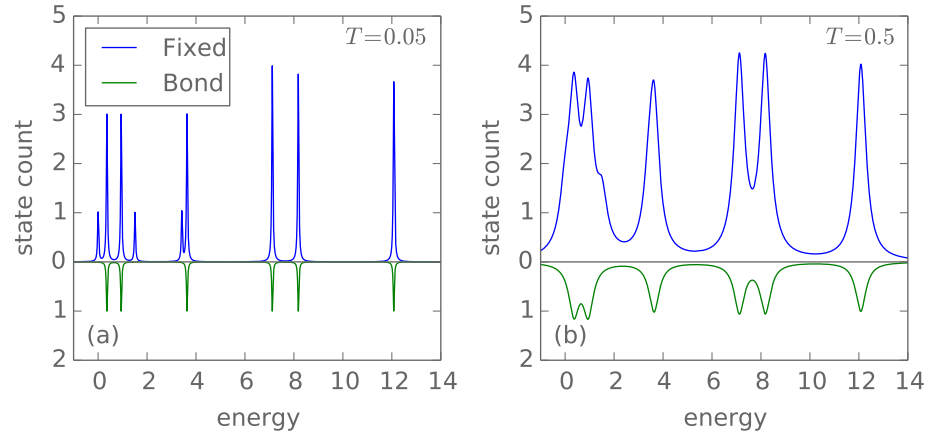


Figure 1.3: Low-energy density of states of a one cell QCA system for both the *fixed charge* and the *bond* model. The *bond* approximation does not reproduce the singlet-triplet splitting.

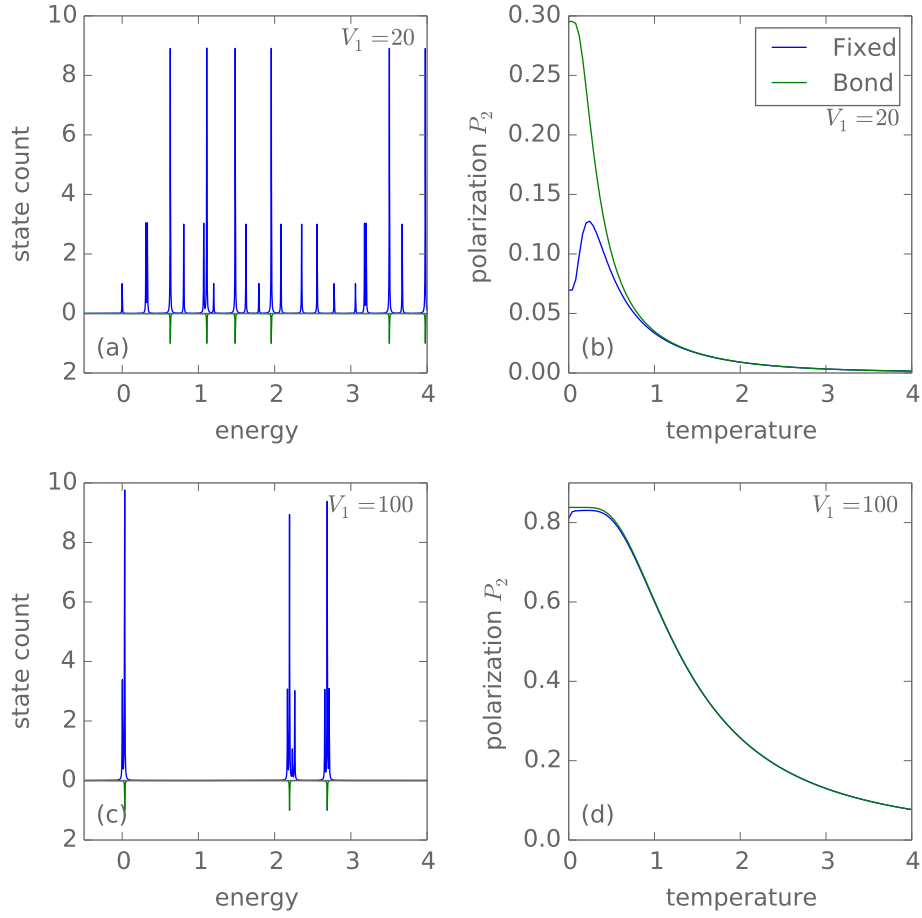


Figure 1.4: The two cell *fixed charge* and *bond* systems at  $V_1 = 20$  and  $V_1 = 100$ . (a)(c) Low-energy density of states. (b)(d) Output polarization  $P_2$  over temperature. For a small Coulomb repulsion the density of states curves look qualitatively very different (a) and the *bond* approximation does not work very well (b). At a larger Coulomb repulsion the density of states curves look much more alike (c) and the *bond* approximation works much better (d).

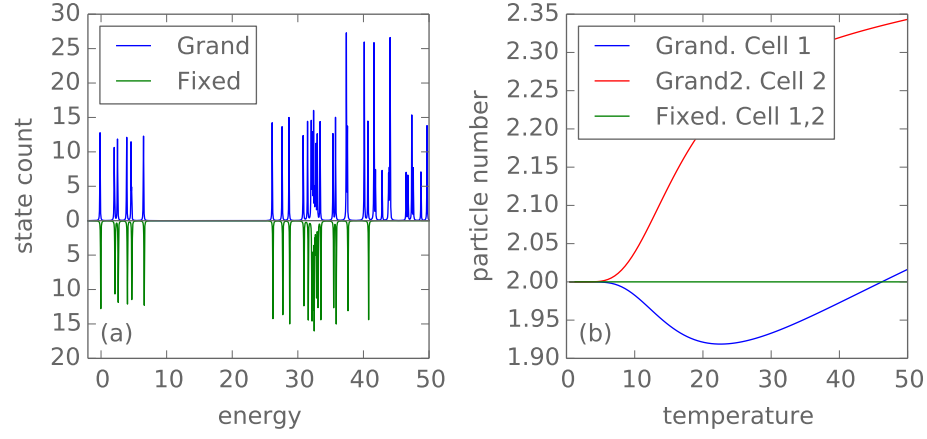


Figure 1.5: (a) Low-energy density of states of the exact *grand canonical* and the approximative *fixed charge* two cell QCA system. For small energies the curves agree perfectly (up to  $E \lesssim 35$ ). (b) Particle number per cell over temperature for the same two cell system. The curves diverge for  $T \gtrsim 5$ .

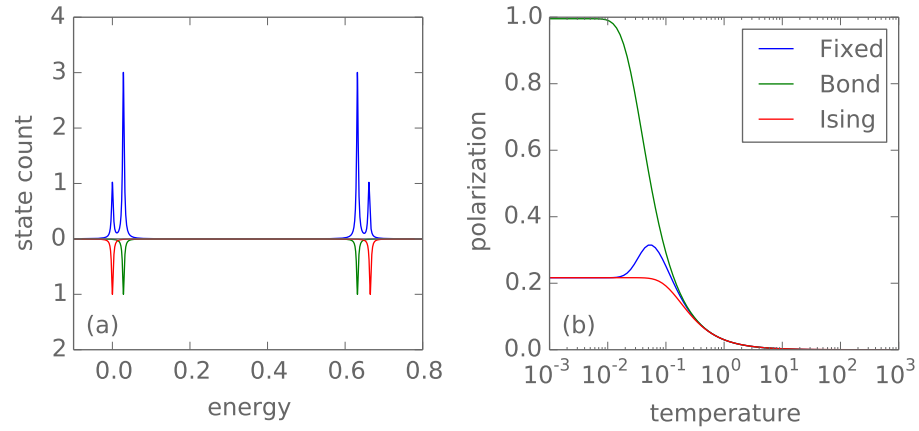


Figure 1.6: ...



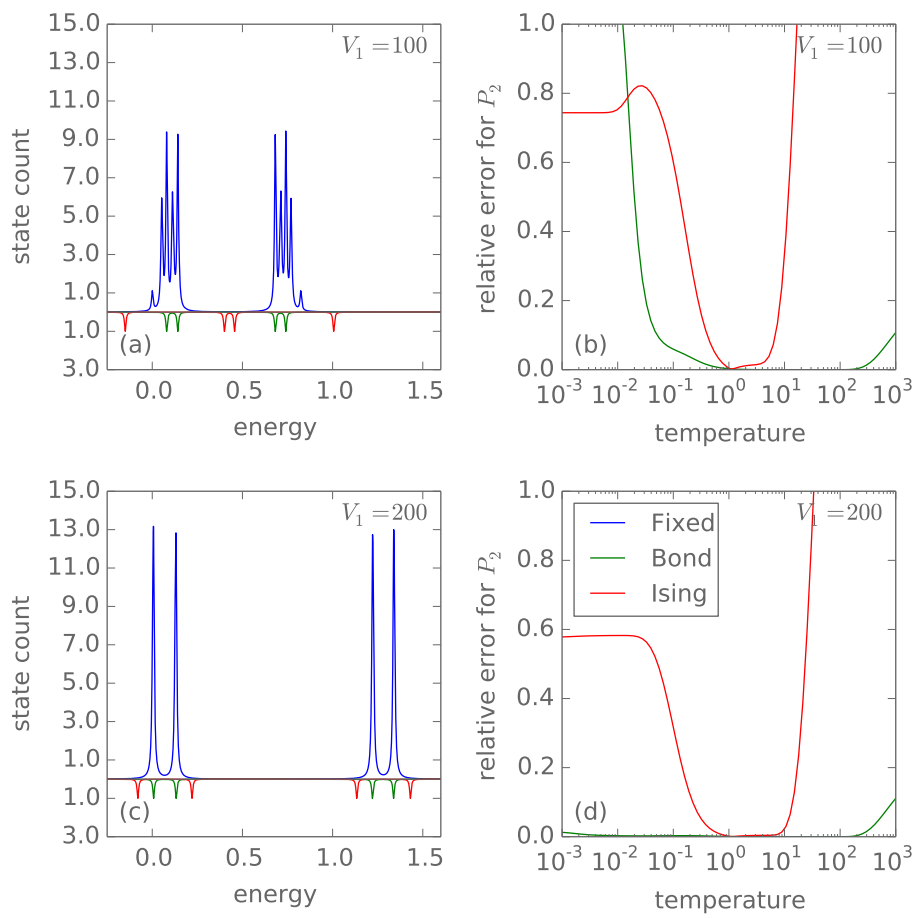


Figure 1.7: ...

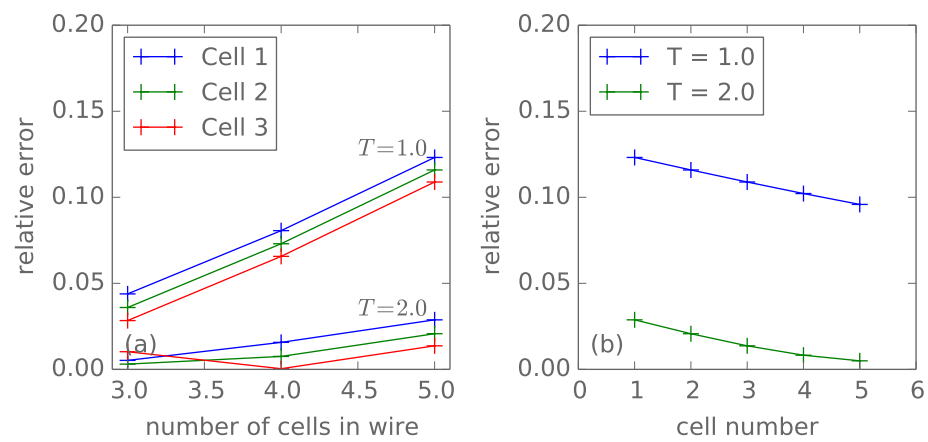


Figure 1.8: ...

# Bibliography

- [1] A. W. Sandvik, “Stochastic series expansion method for quantum Ising models with arbitrary interactions,” *Phys. Rev. E* **68** (Nov, 2003) 056701.  
<http://link.aps.org/doi/10.1103/PhysRevE.68.056701>.